

## Interfacial redox behaviors of sulfide electrolytes in fast-charging all-solid-state lithium metal batteries



Gao-Long Zhu<sup>a,b,c</sup>, Chen-Zi Zhao<sup>b</sup>, Hong Yuan<sup>d</sup>, Bo-Chen Zhao<sup>b</sup>, Li-Peng Hou<sup>b</sup>, Xin-Bing Cheng<sup>b</sup>, Hao-Xiong Nan<sup>b,e</sup>, Yang Lu<sup>b</sup>, Jian Zhang<sup>f</sup>, Jia-Qi Huang<sup>d,\*</sup>, Quan-Bing Liu<sup>e</sup>, Chuan-Xin He<sup>a,\*\*</sup>, Qiang Zhang<sup>b,\*\*\*</sup>

<sup>a</sup> Shenzhen Key Laboratory of Functional Polymer, College of Chemistry and Chemical Engineering, Shenzhen University, Shenzhen, 518000, China

<sup>b</sup> Beijing Key Laboratory of Green Chemical Reaction Engineering and Technology, Department of Chemical Engineering, Tsinghua University, Beijing, 100084, China

<sup>c</sup> Key Laboratory of Optoelectronic Devices and Systems of Ministry of Education and Guangdong Province, College of Optoelectronic Engineering, Shenzhen University, Shenzhen 518060, China

<sup>d</sup> Advanced Research Institute of Multidisciplinary Science, Beijing Institute of Technology, Beijing, 100081, China

<sup>e</sup> School of Chemical Engineering and Light Industry, Guangdong University of Technology, Guangzhou, 510006, China

<sup>f</sup> AAC Technologies Holdings Inc., Nanjing, 10093, China

### ARTICLE INFO

#### Keywords:

All-solid-state lithium metal batteries

Sulfide solid electrolytes

Redox behavior

Cycle stability

Fast charging

### ABSTRACT

Sulfide solid electrolytes offer great opportunities to construct solid-state Li metal batteries with high energy density. The high ionic conductivity of well-developed sulfide electrolytes enables solid-state battery to operate at high current rates. However, sulfide electrolytes exhibit severe decomposition in working cells, constituting a significant obstacle for the practical applications of sulfide solid-state electrolytes. The decomposition behaviors of sulfides are complicated and strongly depend on the electrochemical windows, some of which are even regarded reversible during battery cycling. Herein, we investigate the redox behaviors of Li<sub>7</sub>P<sub>3</sub>S<sub>11</sub> sulfide solid electrolyte under different voltage windows, and their effects on interfacial transport and battery cycle lifetime. Moreover, Li metal | Li<sub>4</sub>Ti<sub>5</sub>O<sub>12</sub> (LTO) batteries are introduced to further probe the role of multiphase redox reactions on interfacial ion conduction. By regulating the redox behaviors of electrolytes through varying working voltage window, Li | LTO metal batteries enable a rapid charge/discharge process in 10 min (6 C) and lifespan of 600 cycles at 1 C with 85% capacity retention. An all-solid-state Li | LTO metal pouch cell is also assembled and exhibits a stable cycling performance with a capacity of 120 mAh g<sup>-1</sup>. This work provides understandings about interfacial redox behaviors of sulfide electrolyte, presenting novel insights in the rational design of future solid-state lithium batteries with high-energy/power-density.

All-solid-state lithium metal batteries (ASSLMBs) are strongly considered as next-generation energy-storage devices because of their exceptional advantages in safety and high energy density [1–9]. The continuous process on the development of solid-state fast ionic conductors enables the battery operation at high rates under room temperature [10–13]. Among these, sulfide-based solid electrolytes have attracted extensive attentions due to their extremely high ionic conductivity (up to 10<sup>-2</sup> S cm<sup>-1</sup> at room temperature), excellent deformability, and a mild low-temperature processability [10,14–18]. However, the full demonstration of practical batteries is a great challenge owing to the slow

lithium-ion transport kinetics at working solid–solid interfaces [2, 19–26]. The sluggish interfacial transport kinetics mainly result from the poor solid–solid contacts [19,27,28], poor chemical [29,30]/electrochemical [31–33] instability at electrode/electrolyte interface, and complex redox behaviors of solid electrolytes in composite electrodes [34–38], thus resulting in a rapid capacity degradation and poor rate performance.

Various strategies aim to improve the interfacial transportation and chemical/electrochemical stability of electrode/electrolyte interfaces, including introducing a soft ionically conductive but electronically

\* Corresponding author.

\*\* Corresponding author.

\*\*\* Corresponding author.

E-mail addresses: [jhuang@bit.edu.cn](mailto:jhuang@bit.edu.cn) (J.-Q. Huang), [hecx@szu.edu.cn](mailto:hecx@szu.edu.cn) (C.-X. He), [zhang-qiang@mails.tsinghua.edu.cn](mailto:zhang-qiang@mails.tsinghua.edu.cn) (Q. Zhang).

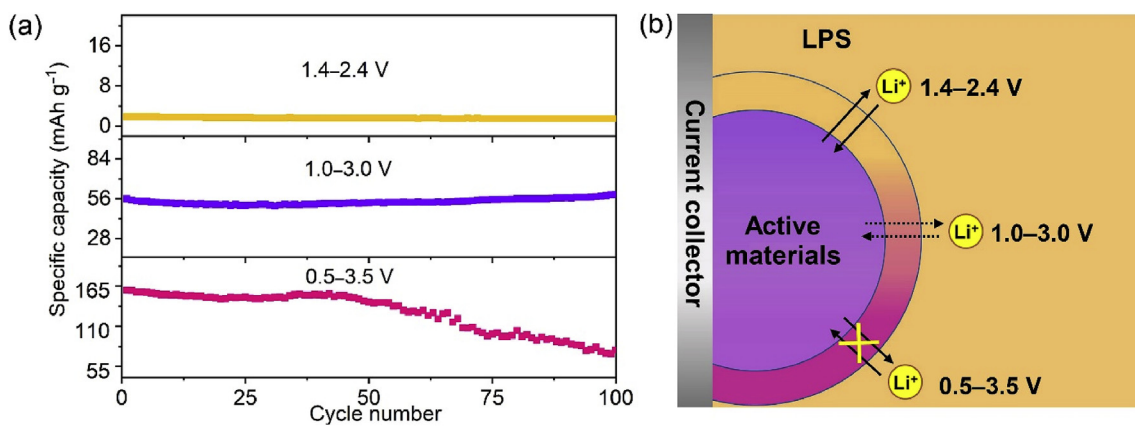


**Fig. 1.** (a) Cycle stability of Li | LPS | LPS cells at various electrochemical windows, (b) schematic of interfacial ion transport between LPS and active materials at various electrochemical windows.

insulative layer between electrode/electrolyte interface [39–43], electrode or electrolyte surface coating [35,44–47], and engineering upgradation to construct conformal contact interfaces [42,46,48–55].

However, the redox behavior of sulfide solid electrolyte in a composite electrode is ubiquitous for ASSLMBs during charge–discharge process, which has been proved by many calculations [56–58] and experiments

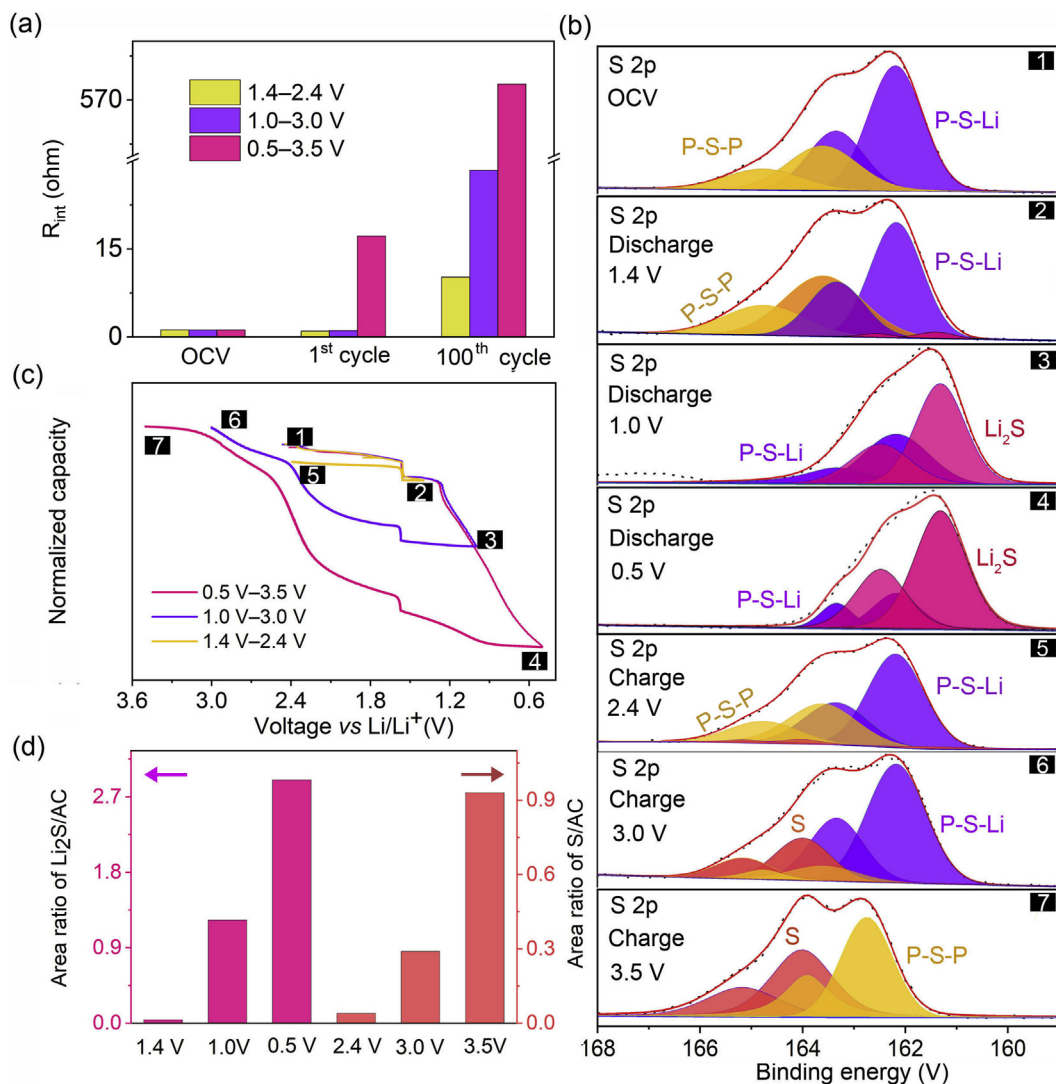


**Fig. 2.** (a)  $R_{int}$  of Li | LPS | LPS cells at various cycles and electrochemical windows. (b) XPS obtained from LPS-CNT cathode at various charge/discharge states. (c) Charge/discharge profiles for reference XPS. OCV represents the open circuit voltage. (d) The peak area ratio of Li<sub>2</sub>S/AC and S/AC in the LPS of LPS-CNT composite cathode under different discharge and charge states. AC represents the peak area of active P-S-P and P-S-Li species.

[37]. The sulfide solid electrolytes endure severe reactions during charge–discharge process and influence lithium-ion transport channels, where the reversible capacity contribution comes from the redox reaction of sulfide electrolytes contacting conductive materials [36–38,59,60]. Furthermore, the passivating nature of redox products, especially the oxidation products contribute to high interfacial impedances [61–63]. However, how the redox reactions of the sulfide electrolytes affect the battery performances and which reaction depth is acceptable for practical batteries are unclear. Therefore, towards rational design of ASSLMBs, it is rewarding to probe the electrochemical redox behaviors of sulfide electrolytes under different electrochemical windows and its corresponding influence on battery performances.

In this contribution, the electrochemical redox behaviors of  $\text{Li}_7\text{P}_3\text{S}_{11}$  (LPS) are investigated comprehensively. The reaction depth of sulfide solid electrolyte depends on the electrochemical window during charge and discharge processes. The reaction products under different voltages are detected and proved to be responsible for the interfacial resistance. The  $\text{Li} \mid \text{LPS} \mid \text{LTO}$  metal cell is used as a model system to evaluate the effect of redox behaviors of sulfide solid electrolyte on battery performances, where the capacity contribution of LTO and LPS can be easily distinguished according to the stable plateau capacity of LTO at 1.55 V. Finally, a practical  $\text{Li} \mid \text{LPS} \mid \text{LTO}$  battery is fully charged/discharged at 6 C and exhibits a long lifespan.

The redox reactions of sulfide solid electrolyte in composite cathodes have a significant effect on the interfacial electrical or ionic transportation at the triple-phase interface among active materials, conductive additives, and solid electrolytes. To probe the reversible decomposition redox reaction of sulfide electrolyte, a composite cathode was constructed with LPS as both active materials and ionic conductors, and carbon nanotubes (CNTs) as electrical conductors. The electrochemical redox depth and capacity contribution of LPS increase with the extension of the charge and discharge cut-off voltages (Fig. 1, Fig. S1). The discharge capacities of LPS increase from 3 to 156 mAh g<sup>-1</sup> when the electrochemical window extends from 1.0 V (1.4–2.4 V) to 3.0 V (0.5–3.5 V), where it serves as active materials in initial cycles. However, the cycle stability of LPS as active materials deteriorates rapidly at an extended voltage window of 0.5–3.5 V with a capacity loss of ~59% after 100 cycles, indicating the severe irreversible decomposition of LPS (Fig. 1a). In comparison, a capacity retention of ~100% is remained after 100 cycles at a voltage range of 1.4–2.4 V. Theoretical calculation reveals that sulfide electrolytes can be oxidized to sulfurous components such as S,  $\text{P}_2\text{S}_5$ , and reduced to  $\text{Li}_3\text{P}$ ,  $\text{Li}_2\text{S}$  [56], most of which affords poor ionic conductivity and leads to retarded interfacial charge transportation. Moreover, the continuous accumulation of low reversible products at LPS/conductive carbon interfaces forms an irreversibly insulated layer, eventually leading to the obstructed interfacial charge transport (Fig. 1b).

The evolution of interfacial charge transport is probed through electrochemical impedance spectroscopy (EIS). As shown in Fig. S2 and Table S1, the high frequency semicircles of the Nyquist plots represent the interfacial resistance, which reflects a combined contribution from both anode–electrolyte interface impedance and interparticle interface impedance in cathode. The cathode–electrolyte interfaces impedance is generally ignored due to compact interface formed under high pressure in battery assembly process. Owing to the relatively high chemical/electrochemical stability of LPS counter to metallic Li, the change in impedance is mainly attributed to the fluctuation of interparticle interfaces impedance in cathode (Table S1). Fig. 2a shows that similar charge transport impedance for three batteries are observed before cycling. After first discharging to different cut-off voltage, the  $R_{\text{int}}$  of batteries reduces except from the battery discharging to a high reduction depth of 0.5 V, which may be ascribed to the interfacial reconstruction at interfaces between LPS and CNTs and thus promote the interfacial contact during redox reaction. Nevertheless, the  $R_{\text{int}}$  value increases from 1.2 to 17.2  $\Omega$  for the cell after first discharging to 0.5 V. In spite of the interfacial reconstruction after first reduction, the passivation layer with

a low ionic/electrical conduction formed due to the generation of insulative  $\text{Li}_2\text{S}$  and  $\text{Li}_3\text{P}$  side products when deeply reduction of LPS, which compensates the superiority in charge transport originated from the interfacial reconstruction and thus results in the enhancement of interfacial resistance. It can be seen that the  $R_{\text{int}}$  values increase to 10.2 and 28.4  $\Omega$  after 100 cycles at the voltage window of 1.4–2.4 and 1.0–3.0 V, respectively, implying that the existence of decomposition products has no obvious influence on the interfacial ionic/electrical transport at these circumstance. The redox behaviors of LPS are electrochemically reversible at a relatively moderate electrochemical windows. However,  $R_{\text{int}}$  grows up to 572.7  $\Omega$  after 100 cycles at the voltage window of 0.5–3.5 V (Fig. 2a). The redox reaction of LPS converts to be low electrochemically reversible or absolutely irreversible after widening the electrochemical window. The generation and accumulation of low conductive  $\text{Li}_2\text{S}$  and S and finally the formation of insulative layers at LPS/carbon interfaces during cycling impede the interfacial ion transport in composite cathode. Therefore, it is very important for the selection of an appropriate electrochemical window to achieve highly reversible redox reaction of sulfides and to finally maintain stable interfacial charge transport.

In order to further investigate the effects of redox behavior of sulfide solid electrolytes on interfacial lithium-ion transport, the redox products of LPS at various discharge/charge states were characterized by XPS (Fig. 2b) based on three charge-discharge processes under different voltage windows (Fig. 2c). The decomposition products of LPS at different charge/discharge cut-off voltages were investigated and their S 2p XPS spectra were fitted with spin-orbit coupled  $2p^{3/2}$  and  $2p^{1/2}$  doublets. There are two pairs of characteristic peaks for pristine LPS electrolyte at fresh electrode, which are related to the bridging sulfur P–S–P (163.3 eV) and non-bridging sulfur P–S–Li (162.1 eV), respectively [36]. Notably, one pair of peaks appear at the binding energy of ~161.2 eV with the reduction of LPS, which is attributed to electron-rich  $\text{S}^{2-}$  species in  $\text{Li}_2\text{S}$  [36]. Moreover, the peak intensity increases as the proceeding of discharging, indicating the increase of low conductive  $\text{Li}_2\text{S}$  reduction products (Fig. 2b). Meanwhile, the content of active P–S–P and P–S–Li species that contribute to the Li ion conduction decreased. When this decomposition products are converted to be oxidation states (charged to 2.4, 3.0, and 3.5 V, respectively), it is interesting that oxidized elemental sulfur presents and its content increases with the rise of oxidation degree. The XPS peaks area ratios of  $\text{Li}_2\text{S}/\text{active species (AC)}$  of P–S–P and P–S–Li and S/AC are shown in Fig. 2d. In the discharging process, the ratio of  $\text{Li}_2\text{S}/\text{AC}$  increases from 0.04 to 2.9, and the ratio of S/AC increases from 0.04 to 0.93 in charging process. These indicating that the main components of the reduction products should be  $\text{Li}_3\text{P}$ ,  $\text{Li}_2\text{S}$  and the oxidation products should be S,  $\text{P}_2\text{S}_5$ . Moreover, the reduction and oxidation products enable to circulate reversibly during charging and discharging. However, elemental sulfur is an ionic/electrical insulator, which can also deteriorate charge conduction and lead to high interfacial resistance. Additionally, the intrinsic insulative nature of  $\text{Li}_2\text{S}$  and S decomposition products also enhances the electrochemical redox overpotential for LPS redox reaction and thus, resulting in irreversible conversion between insulative  $\text{Li}_2\text{S}$  and S and eventually leading their accumulation at the LPS/carbon interface during cycling at widening electrochemical window [36,57].

As a star anode material for fast-charging Li-ion batteries, LTO can be employed as a model electrode material to evaluate electrode interface reaction process due to the exceedingly flat voltage plateau at 1.55 V (LTO vs. Li), which can be easily distinguished from electrode reactions. Herein, the LTO composite cathode was prepared to investigate the effect of LPS redox behaviors on lithiation/delithiation process in a practical working battery (in which Li metal as anode while LPS as solid electrolyte) through the blending of LTO active materials, LPS electrolytes and conductive CNTs. Ion transportation capability in composite cathodes is determined by sulfide electrolytes and their redox products during charge/discharge process, consequently affecting the specific capacity and voltage polarization of LTO active materials. The corresponding capacity of LTO is calculated based on the capacity covers the plateau

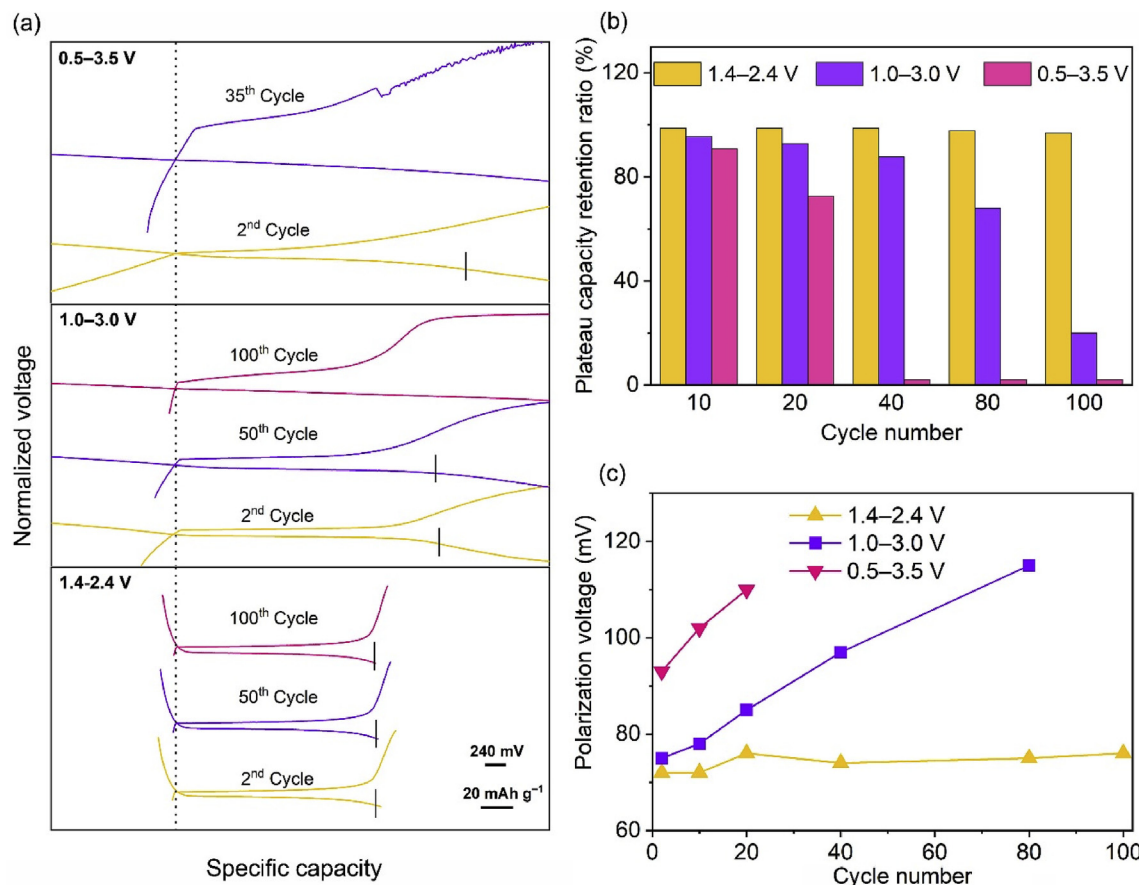


**Fig. 3.** (a) Plateau capacity of LTO for Li | LPS | LTO cells at various electrochemical windows for different cycles, the legend labeled  $20 \text{ mAh g}^{-1}$  is the scale bar of horizontal line and the legend labeled  $240 \text{ mV}$  is the scale bar of vertical line. (b) Capacity retention ratio of discharge plateau capacity of LTO. (c) Polarization voltage of Li | LPS | LTO cells vs cycle number for 1 C at different electrochemical windows.

voltage within  $\pm 90 \text{ mV}$  range. As shown in Fig. 3a, unambiguous charge/discharge plateaus are observed for all LTO batteries. The discharge capacity exceeds the theoretical capacity of LTO, which is ascribed to the contribution of discharged LPS. This result demonstrates the occurrence of LPS redox behaviors in a practical cathode. Deducting the capacity contribution of LPS, LTO exhibits an equal plateau capacity of about  $120 \text{ mAh g}^{-1}$  at various electrochemical windows after two cycles. However, the polarization of LTO-based batteries increases with the extension of voltage window, indicating the internal resistance of battery increases with the boost of LPS reaction depth. The difference in polarization further validates that redox behaviors of LPS have a significant influence on charge transport in LTO composite cathode.

In fact, the irreversibility of LPS redox results in the continuous interface destruction owing to the accumulation of decomposition products during repeated cycling. The specific capacity of LTO gradually reduces with battery cycling at a widened electrochemical window (Fig. 3b), which is attributed to the generation of plenty of irreversible decomposition products and leads to enhanced interfacial resistance and high redox overpotential. The characteristic discharge plateau of LTO even disappears after 100 cycles and 35 cycles at an extended voltage window of 1–3 and 0.5–3.5 V, respectively (Fig. 3b). Although the cells at extended windows exhibit higher specific capacities due to the capacity contribution of LPS, the Li | LPS | LTO metal cells finally fail in the 165th and 35th cycle at voltage window of 1–3 and 0.5–3.5 V (Fig. S3) due to the ion transport pathways are completely blocked by the accumulation of redox products during repeated cycling. In contrast, the capacity of LTO still remains 97% after 100 cycles at a voltage window of 1.4–2.4 V, implying negligible interface destruction resulted from the mild decomposition of LPS and their redox reversibility at a limited

electrochemical window. These results also proved by the change in voltage polarization (Fig. 3c). The polarization overpotential remains 75 mV after 100th cycles and there is no obvious voltage fluctuation during cycling at a limited electrochemical window, demonstrating the accumulation of irreversible and low conductive side products is negligible. As aforementioned, detrimental decomposition products sharply generate and accumulate with the increase of reaction degree when widening electrochemical window. Consequently, the polarization overpotential progressively increases from 75 to 115 mV after 80th cycles at a moderate electrochemical window of 1.0–3.0 V. While, the polarization voltage quickly increases from 93 mV (first cycle) to 110 mV (20th cycle) at a voltage window of 0.5–3.5 V and the battery finally failed after 35 cycles. In a working sulfide-based solid battery, sulfides served as ionic conductors to ensure the fast ionic transport in a composite cathode. Despite the possibility of LPS redox reaction contributes to enhanced discharge capacity, the formation of irreversible side products induces the rapid degradation of electrode/electrolyte interface and enhances the resistance of interfacial charge conduction. Meanwhile, the constant accumulation of detrimental decomposition products results in the formation of insulative layer and finally passivates electrode/electrolyte interface. Therefore, a suitable electrochemical window is imperative to balance between discharge capacity and cycle stability.

Fast charging, as one of the core technologies of state-of-the-art rechargeable batteries, has drawn extensive interests to mitigate the range anxiety and exhibits a great market prospect. It is important to realize fast charging in solid-state lithium batteries because of the intrinsic stability and safety properties of ASSLMBs. However, the rate performance of a battery is extraordinarily sensitive for charge conduction, which relies on not only the ability of electrode active materials to

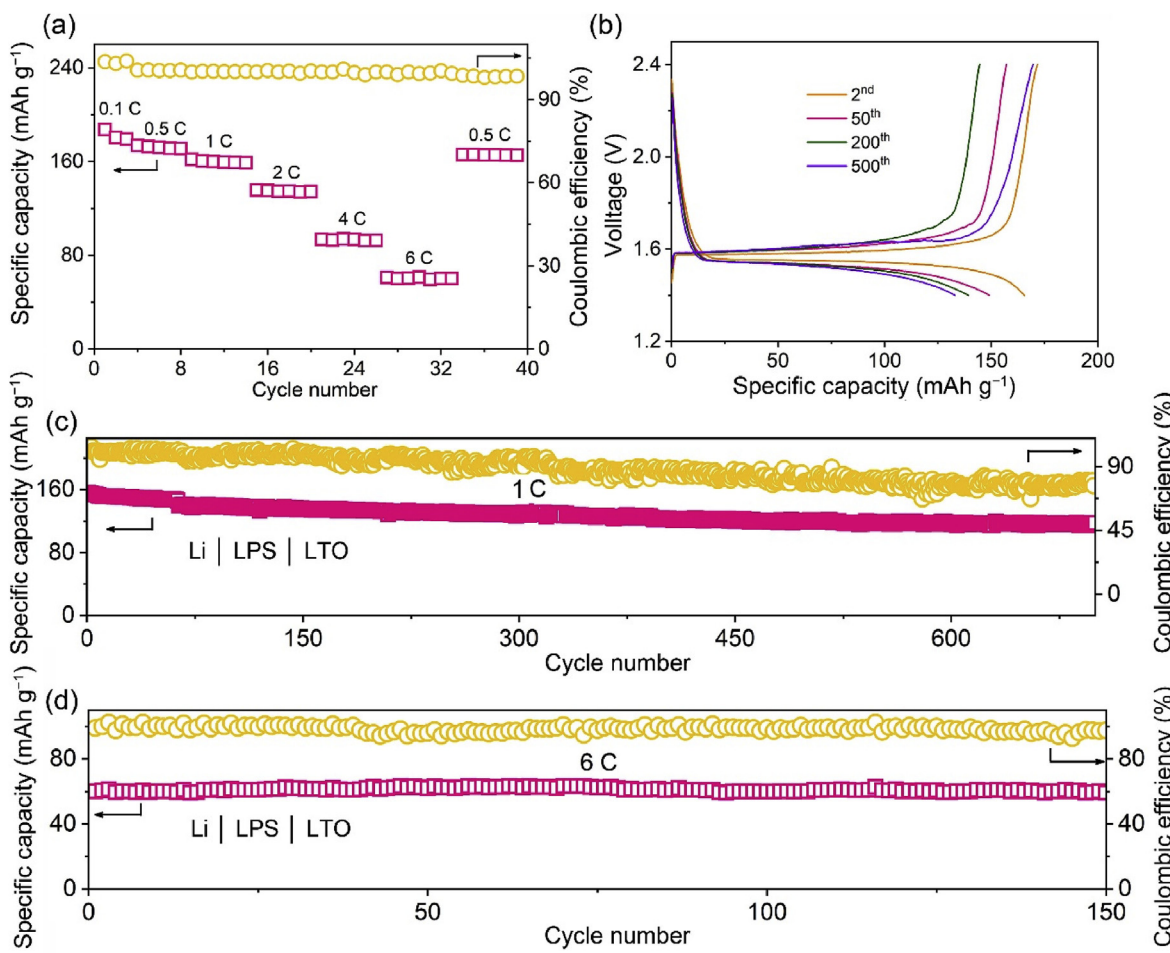


**Fig. 4.** (a) Rate performances, (b) charge-discharge profiles and (c) cycle stability of Li | LPS | LTO cells at 1.4–2.4 V at 1 C. (d) Cycle stability of the cells at 1.4–2.4 V at 6 C.

rapidly respond to acceptance of Li ions but also the fast transport of Li ions at electrode/electrolyte interface. To further validate the interface stability, the rate performance of all-solid-state LTO-based cell was investigated at a limited electrochemical window of 1.4–2.4 V (Fig. 4a). With a LTO loading of 1.3 mg cm<sup>-2</sup>, the cell delivers an initial discharge capacity of 172 mAh g<sup>-1</sup> at 0.1 C (1 C = 175 mAh g<sup>-1</sup>). While increasing the current density to 0.5, 1.0, 2.0, 4.0, and 6.0 C, an unprecedented reversible capacity of 169, 158, 134, 92, and 62 mAh g<sup>-1</sup> is maintained, respectively. After converting current density back to 0.5 C, a reversible discharge capacity of 169 mAh g<sup>-1</sup> is recovered after ultrahigh rate test, further suggesting negligible interface destruction for ion transport.

Furthermore, the reversibility of LPS redox at a limited electrochemical window also regulates the long-term cycling stability of LTO-based cells at high current density of 1.0 and 6.0 C (Fig. 4b and c). The cell exhibits an excellent stability with 85% of initial capacity after 600 cycles at 1 C. Surprisingly, increasing current density to 6.0 C, a capacity retention of 98% (59.5 mAh g<sup>-1</sup>) after 150 cycles is demonstrated. These results indicated the possibility of achieving fast charging of LTO batteries under the premise of stable interfacial capability in charge transfer. In addition, a LTO-based all-solid-state pouch cell with a size of 30 × 30 mm was also assembled. The pouch cell exhibits excellent rate performance and an outstanding cycle stability with a capacity retention of 120 mAh g<sup>-1</sup> at 1 C after 20 cycles is also observed (Fig. S4), which illustrates the practical application potential of sulfide-based LTO solid electrode in the field of fast charging.

In summary, the electrochemical redox behaviors of sulfide solid electrolyte and their influences on electrochemical performances at

various electrochemical windows were investigated comprehensively. The redox decomposition of LPS and the irreversible side products (Li<sub>2</sub>S and S) is responsible for the interface charge resistance. A serious redox reaction of LPS occur at a wide electrochemical window and the amount of side products increases with the redox reaction depth. Moreover, the redox reaction of solid electrolyte is a continuous deterioration process. The generation and accumulation of decomposition products result in the increased interfacial resistance and enlarged polarization, finally forming an insulative layer at the electrode/electrolyte interface and rendering a fast capacity degradation. In all-solid-state Li | LTO metal batteries, the operation at a limited electrochemical window of 1.4–2.4 V achieved excellent rate performances at an elevated rate of 6 C with 98% capacity retention after 150 cycles. Furthermore, a high capacity retention of 85% was also maintained after 600 cycles at 1 C, which exhibits outstanding fast-charging capability of sulfide-based all-solid-state battery without obvious interfacial deterioration. This work not only promotes the understanding on redox behaviors of sulfide electrolytes at electrode/electrolyte interface, also provides a fresh insight to the possibility of fast-charging solid-state batteries through electrochemical regulation and interfacial engineering.

#### Declaration of competing interest

The authors declare that they have no known competing financial interests or personal relationships that could have appeared to influence the work reported in this paper.

## CRediT authorship contribution statement

**Gao-Long Zhu:** Methodology, Investigation, Data curation, Writing - original draft. **Chen-Zi Zhao:** Investigation, Data curation, Writing - original draft. **Hong Yuan:** Methodology, Data curation, Validation. **Bo-Chen Zhao:** Investigation. **Li-Peng Hou:** Investigation. **Xin-Bing Cheng:** Validation, Writing - review & editing. **Hao-Xiong Nan:** Investigation. **Yang Lu:** Investigation, Writing - review & editing. **Jian Zhang:** Writing - review & editing. **Jia-Qi Huang:** Supervision, Conceptualization, Writing - review & editing. **Quan-Bing Liu:** Writing - review & editing. **Chuan-Xin He:** Supervision, Conceptualization, Writing - review & editing. **Qiang Zhang:** Supervision, Conceptualization, Writing - review & editing.

## Acknowledgements

This work was supported by National Key Research and Development Program (2016YFA0202500 and 2016YFA0200102), National Natural Science Foundation of China (21676160, 21825501, 21805161, 21808121, and U1801257), and China Postdoctoral Science Foundation (2018M631480).

## Appendix A. Supplementary data

Supplementary data to this article can be found online at <https://doi.org/10.1016/j.ensm.2020.05.017>.

## References

- [1] K.H. Park, Q. Bai, D.H. Kim, D.Y. Oh, Y. Zhu, Y. Mo, Y.S. Jung, Design strategies, practical considerations, and new solution processes of sulfide solid electrolytes for all-solid-state batteries, *Adv. Energy Mater.* 8 (2018) 1800035.
- [2] W. Chen, T. Lei, C. Wu, M. Deng, C. Gong, K. Hu, Y. Ma, L. Dai, W. Lv, W. He, X. Liu, J. Xiong, C. Yan, Designing safe electrolyte systems for a high-stability lithium–sulfur battery, *Adv. Energy Mater.* 8 (2018) 1702348.
- [3] J. Janek, W.G. Zeier, A solid future for battery development, *Nat. Energy* 1 (2016) 16141.
- [4] S. Xia, X. Wu, Z. Zhang, Y. Cui, W. Liu, Practical challenges and future perspectives of all-solid-state lithium–metal batteries, *Inside Chem.* 5 (2018) 753.
- [5] C.-Z. Zhao, X.-Q. Zhang, X.-B. Cheng, R. Zhang, R. Xu, P.-Y. Chen, H.-J. Peng, J.-Q. Huang, Q. Zhang, An anion-immobilized composite electrolyte for dendrite-free lithium metal anodes, *Proc. Natl. Acad. Sci. Unit. States Am.* 114 (2017) 11069.
- [6] H. Huo, Y. Chen, J. Luo, X. Yang, X. Guo, X. Sun, Rational design of hierarchical “ceramic-in-polymer” and “polymer-in-ceramic” electrolytes for dendrite-free solid-state batteries, *Adv. Energy Mater.* 9 (2019) 1804004.
- [7] M. Li, J. Lu, Z. Chen, K. Amine, 30 Years of lithium-ion batteries, *Adv. Mater.* 30 (2018) 1800561.
- [8] Q. Zhao, X. Liu, S. Stalin, K. Khan, L.A. Archer, Solid-state polymer electrolytes with in-built fast interfacial transport for secondary lithium batteries, *Nat. Energy* 4 (2019) 365.
- [9] X. Huang, Y. Lu, Z. Song, T. Xiu, M.E. Badding, Z. Wen, Preparation of dense Ta-Li2O/MgO composite Li-ion solid electrolyte: sintering, microstructure, performance and the role of MgO, *J. Energy Chem.* 39 (2019) 8.
- [10] Y. Kato, S. Hori, T. Saito, K. Suzuki, M. Hirayama, A. Mitsui, M. Yonemura, H. Iba, R. Kanno, High-power all-solid-state batteries using sulfide superionic conductors, *Nat. Energy* 1 (2016) 16030.
- [11] Y. Liu, Y. Zhu, Y. Cui, Challenges and opportunities towards fast-charging battery materials, *Nat. Energy* 4 (2019) 540.
- [12] S. Chen, D. Xie, G. Liu, J.P. Mwizerwa, Q. Zhang, Y. Zhao, X. Xu, X. Yao, Sulfide solid electrolytes for all-solid-state lithium batteries: structure, conductivity, stability and application, *Energy Storage Mater.* 14 (2018) 58.
- [13] Y. Jiang, Z. Wang, C. Xu, W. Li, Y. Li, S. Huang, Z. Chen, B. Zhao, X. Sun, D.P. Wilkinson, J. Zhang, Atomic layer deposition for improved lithophilicity and solid electrolyte interface stability during lithium plating, *Energy Storage Mater.* 28 (2020) 17.
- [14] N. Kamaya, K. Homma, Y. Yamakawa, M. Hirayama, R. Kanno, M. Yonemura, T. Kamiyama, Y. Kato, S. Hama, K. Kawamoto, A. Mitsui, A lithium superionic conductor, *Nat. Mater.* 10 (2011) 682.
- [15] Y. Seino, T. Ota, K. Takada, A. Hayashi, M. Tatsumisago, A sulphide lithium super ion conductor is superior to liquid ion conductors for use in rechargeable batteries, *Energy Environ. Sci.* 7 (2014) 627.
- [16] L. Liu, J. Xu, S. Wang, F. Wu, H. Li, L. Chen, Practical evaluation of energy densities for sulfide solid-state batteries, *eTransportation* 1 (2019) 100010.
- [17] R. Chen, Q. Li, X. Yu, L. Chen, H. Li, Approaching practically Accessible solid-state batteries: stability issues related to solid electrolytes and interfaces, *Chem. Rev.* (2019), <https://doi.org/10.1021/acs.chemrev.9b00268>.
- [18] M.A. Kraft, S. Ohno, T. Zinkevich, R. Koerver, S.P. Culver, T. Fuchs, A. Senyshyn, S. Indris, B.J. Morgan, W.G. Zeier, Inducing high ionic conductivity in the lithium superionic Argyrodite  $\text{Li}_{6+x}\text{P}_{1-x}\text{Ge}_x\text{S}_5\text{I}$  for all-solid-state batteries, *J. Am. Chem. Soc.* 140 (2018) 16330.
- [19] L. Xu, S. Tang, Y. Cheng, K. Wang, J. Liang, C. Liu, Y.-C. Cao, F. Wei, L. Mai, Interfaces in solid-state lithium batteries, *Joule* 2 (2018) 1991.
- [20] Y.S. Jung, D.Y. Oh, Y.J. Nam, K.H. Park, Issues and challenges for bulk-type all-solid-state rechargeable lithium batteries using sulfide solid electrolytes, *Isr. J. Chem.* 55 (2015) 472.
- [21] C. Wang, Y. Zhao, Q. Sun, X. Li, Y. Liu, J. Liang, X. Li, X. Lin, R. Li, K.R. Adair, L. Zhang, R. Yang, S. Lu, X. Sun, Stabilizing interface between  $\text{Li}_{10}\text{SnP}_2\text{S}_{12}$  and Li metal by molecular layer deposition, *Nanomater. Energy* 53 (2018) 168.
- [22] F. Du, N. Zhao, Y. Li, C. Chen, Z. Liu, X. Guo, All solid state lithium batteries based on lamellar garnet-type ceramic electrolytes, *J. Power Sources* 300 (2015) 24.
- [23] R. Koerver, W. Zhang, L. de Biasi, S. Schweidler, A.O. Kondrakov, S. Kolling, T. Brezesinski, P. Hartmann, W.G. Zeier, J. Janek, Chemo-mechanical expansion of lithium electrode materials—the route to mechanically optimized all-solid-state batteries, *Energy Environ. Sci.* 11 (2018) 2142.
- [24] L.-P. Hou, H. Yuan, C.-Z. Zhao, L. Xu, G.-L. Zhu, H.-X. Nan, X.-B. Cheng, Q.-B. Liu, C.-X. He, J.-Q. Huang, Q. Zhang, Improved interfacial electronic contacts powering high sulfur utilization in all-solid-state lithium–sulfur batteries, *Energy Storage Mater.* 25 (2019) 436.
- [25] X.-B. Cheng, C.-Z. Zhao, Y.-X. Yao, H. Liu, Q. Zhang, Recent Advances in energy chemistry between solid-state electrolyte and safe lithium-metal anodes, *Inside Chem.* 5 (2019) 74.
- [26] R. Xu, C. Yan, Y. Xiao, M. Zhao, H. Yuan, J.-Q. Huang, The reduction of interfacial transfer barrier of Li ions enabled by inorganics-rich solid-electrolyte interphase, *Energy Storage Mater.* 28 (2019) 401.
- [27] H. Zhang, U. Oteo, X. Judez, G.G. Eshetu, M. Martinez-Ibañez, J. Carrasco, C. Li, M. Armand, Designer anion enabling solid-state lithium-sulfur batteries, *Joule* 3 (2019) 1689.
- [28] S. Yu, D.J. Siegel, Grain boundary softening: a potential mechanism for lithium metal penetration through stiff solid electrolytes, *ACS Appl. Mater. Interfaces* 10 (2018) 38151.
- [29] S. Wenzel, S. Randau, T. Leichtweiss, D.A. Weber, J. Sann, W.G. Zeier, J. Janek, Direct observation of the interfacial instability of the fast ionic conductor  $\text{Li}_{10}\text{GeP}_2\text{S}_{12}$  at the lithium metal anode, *Chem. Mater.* 28 (2016) 2400.
- [30] S. Wenzel, D.A. Weber, T. Leichtweiss, M.R. Busche, J. Sann, J. Janek, Interphase formation and degradation of charge transfer kinetics between a lithium metal anode and highly crystalline  $\text{Li}_7\text{P}_3\text{S}_{11}$  solid electrolyte, *Solid State Ionics* 286 (2016) 24.
- [31] L. Sang, K.L. Bassett, F.C. Castro, M.J. Young, L. Chen, R.T. Haasch, J.W. Elam, V.P. Dravid, R.G. Nuzzo, A.A. Gewirth, Understanding the effect of interlayers at the thiophosphate solid electrolyte/lithium interface for all-solid-state Li batteries, *Chem. Mater.* 30 (2018) 8747.
- [32] S.P. Ong, Y. Mo, W.D. Richards, L. Miar, H.S. Lee, G. Ceder, Phase stability, electrochemical stability and ionic conductivity of the  $\text{Li}_{10-x}\text{MPX}_{12}$  ( $M = \text{Ge}, \text{Si}, \text{Sn}, \text{Al or P, and } X = \text{O, S or Se}$ ) family of superionic conductors, *Energy Environ. Sci.* 6 (2013) 148.
- [33] J. Kasemchainan, S. Zekoll, D. Spencer Jolly, Z. Ning, G.O. Hartley, J. Marrow, P.G. Bruce, Critical stripping current leads to dendrite formation on plating in lithium anode solid electrolyte cells, *Nat. Mater.* 18 (2019) 1105.
- [34] T. Swamy, X. Chen, Y.-M. Chiang, Electrochemical redox behavior of Li ion conducting sulfide solid electrolytes, *Chem. Mater.* 31 (2019) 707.
- [35] X. Yao, N. Huang, F. Han, Q. Zhang, H. Wan, J.P. Mwizerwa, C. Wang, X. Xu, High-performance all-solid-state lithium-sulfur batteries enabled by Amorphous sulfur-coated reduced graphene oxide cathodes, *Adv. Energy Mater.* 7 (2017) 1602923.
- [36] Y. Zhang, R. Chen, T. Liu, B. Xu, X. Zhang, L. Li, Y. Lin, C.-W. Nan, Y. Shen, High capacity and superior cyclic performances of all-solid-state lithium batteries enabled by a glass-ceramics solo, *ACS Appl. Mater. Interfaces* 10 (2018) 10029.
- [37] F. Han, T. Gao, Y. Zhu, K.J. Gaskell, C. Wang, A battery made from a single material, *Adv. Mater.* 27 (2015) 3473.
- [38] T. Hakari, M. Nagao, A. Hayashi, M. Tatsumisago, All-solid-state lithium batteries with  $\text{Li}_3\text{PS}_4$  glass as active material, *J. Power Sources* 293 (2015) 721.
- [39] N. Ohta, K. Takada, L. Zhang, R. Ma, M. Osada, T. Sasaki, Enhancement of the high-rate capability of solid-state lithium batteries by nanoscale interfacial modification, *Adv. Mater.* 18 (2006) 2226.
- [40] Q. Zhang, J.P. Mwizerwa, H. Wan, L. Cai, X. Xu, X. Yao,  $\text{Fe}_3\text{S}_4 @ \text{Li}_7\text{P}_3\text{S}_{11}$  nanocomposites as cathode materials for all-solid-state lithium batteries with improved energy density and low cost, *J. Mater. Chem. A* 5 (2017) 23919.
- [41] D.Y. Oh, A.R. Ha, J.E. Lee, S.H. Jung, G. Jeong, W. Cho, K.S. Kim, Y.S. Jung, Wet-chemical tuning of  $\text{Li}_{3-x}\text{PS}_4$  ( $0 \leq x \leq 0.3$ ) enabled by dual solvents for all-solid-state lithium-ion batteries, *ChemSusChem* 12 (2019) 1.
- [42] D.Y. Oh, Y.J. Nam, K.H. Park, S.H. Jung, K.T. Kim, A.R. Ha, Y.S. Jung, Slurry-fabricable  $\text{Li}^{+}$ -Conductive polymeric binders for practical all-solid-state lithium-ion batteries enabled by solvate ionic liquids, *Adv. Energy Mater.* 9 (2019) 1802927.
- [43] A. Miura, N.C. Rosero-Navarro, A. Sakuda, K. Tadanaga, N.H.H. Phuc, A. Matsuda, N. Machida, A. Hayashi, M. Tatsumisago, Liquid-phase syntheses of sulfide electrolytes for all-solid-state lithium battery, *Nat. Rev. Chem.* 3 (2019) 189.
- [44] Z. Lin, Z. Liu, N.J. Dudney, C. Liang, Lithium superionic sulfide cathode for all-solid lithium–sulfur batteries, *ACS Nano* 7 (2013) 2829.
- [45] A. Sakuda, A. Hayashi, M. Tatsumisago, Interfacial observation between  $\text{LiCoO}_2$  electrode and  $\text{Li}_2\text{S}-\text{P}_2\text{S}_5$  solid electrolytes of all-solid-state lithium secondary batteries using transmission electron microscopy, *Chem. Mater.* 22 (2010) 949.

- [46] F. Han, J. Yue, X. Fan, T. Gao, C. Luo, Z. Ma, L. Suo, C. Wang, High-performance all-solid-state lithium–sulfur battery enabled by a mixed-conductive Li<sub>2</sub>S nanocomposite, *Nano Lett.* 16 (2016) 4521.
- [47] D. Cao, Y. Zhang, A.M. Nolan, X. Sun, C. Liu, J. Sheng, Y. Mo, Y. Wang, H. Zhu, Stable thiophosphate-based all-solid-state lithium batteries through conformally interfacial nanocoating, *Nano Lett.* 20 (2019) 1483.
- [48] M. He, Z. Cui, F. Han, X. Guo, Construction of conductive and flexible composite cathodes for room-temperature solid-state lithium batteries, *J. Alloys Compd.* 762 (2018) 157.
- [49] D.H. Kim, D.Y. Oh, K.H. Park, Y.E. Choi, Y.J. Nam, H.A. Lee, S.-M. Lee, Y.S. Jung, Infiltration of solution-processable solid electrolytes into conventional Li-Ion-Battery electrodes for all-solid-state Li-ion batteries, *Nano Lett.* 17 (2017) 3013.
- [50] R. Xu, J. Yue, S. Liu, J. Tu, F. Han, P. Liu, C. Wang, Cathode-supported all-solid-state lithium–sulfur batteries with high cell-level energy density, *ACS Energy Lett.* 4 (2019) 1073.
- [51] Y. Zhang, Y. Shi, X.-C. Hu, W.-P. Wang, R. Wen, S. Xin, Y.-G. Guo, A 3D lithium/carbon fiber anode with sustained electrolyte contact for solid-state batteries, *Adv. Energy Mater.* 10 (2019) 1903325.
- [52] D.Y. Oh, D.H. Kim, S.H. Jung, J.G. Han, N.S. Choi, Y.S. Jung, Single-step wet-chemical fabrication of sheet-type electrodes from solid-electrolyte precursors for all-solid-state lithium-ion batteries, *J. Mater. Chem. A* 5 (2017) 20771.
- [53] S.Z. Zhang, X.H. Xia, D. Xie, R.C. Xu, Y.J. Xu, Y. Xia, J.B. Wu, Z.J. Yao, X.L. Wang, J.P. Tu, Facile interfacial modification via in-situ ultraviolet solidified gel polymer electrolyte for high-performance solid-state lithium ion batteries, *J. Power Sources* 409 (2019) 31.
- [54] S. Liu, X. Xia, S. Deng, D. Xie, Z. Yao, L. Zhang, S. Zhang, X. Wang, J. Tu, In situ solid electrolyte interphase from spray quenching on molten Li: a new way to construct high-performance lithium-metal anodes, *Adv. Mater.* 31 (2019) 1806470.
- [55] L. Zhou, K.-H. Park, X. Sun, F. Lalère, T. Adermann, P. Hartmann, L.F. Nazar, Solvent-engineered design of Argyrodite Li<sub>6</sub>PS<sub>5</sub>X (X = Cl, Br, I) solid electrolytes with high ionic conductivity, *ACS Energy Lett.* 4 (2019) 265.
- [56] Y. Zhu, X. He, Y. Mo, Origin of outstanding stability in the lithium solid electrolyte materials: insights from thermodynamic Analyses based on first-principles calculations, *ACS Appl. Mater. Interfaces* 7 (2015) 23685.
- [57] F. Han, Y. Zhu, X. He, Y. Mo, C. Wang, Electrochemical stability of Li<sub>10</sub>GeP<sub>2</sub>S<sub>12</sub> and Li<sub>7</sub>La<sub>3</sub>Zr<sub>2</sub>O<sub>12</sub> solid electrolytes, *Adv. Energy Mater.* 6 (2016) 1501590.
- [58] Y. Zhu, X. He, Y. Mo, Strategies based on nitride materials chemistry to stabilize Li metal anode, *Adv. Sci.* 4 (2017), 1600517.
- [59] T. Hakari, Y. Sato, S. Yoshimi, A. Hayashi, M. Tatsumisago, Favorable carbon conductive additives in Li<sub>3</sub>PS<sub>4</sub> composite positive electrode prepared by ball-milling for all-solid-state lithium batteries, *J. Electrochem. Soc.* 164 (2017) A2804.
- [60] T. Hakari, M. Deguchi, K. Mitsuhashi, T. Ohta, K. Saito, Y. Orikasa, Y. Uchimoto, Y. Kowada, A. Hayashi, M. Tatsumisago, Structural and electronic-state changes of a sulfide solid electrolyte during the Li deinsertion–insertion processes, *Chem. Mater.* 29 (2017) 4768.
- [61] W. Zhang, T. Leichtweiß, S.P. Culver, R. Koerver, D. Das, D.A. Weber, W.G. Zeier, J. Janek, The detrimental effects of carbon additives in Li<sub>10</sub>GeP<sub>2</sub>S<sub>12</sub>-based solid-state batteries, *ACS Appl. Mater. Interfaces* 9 (2017) 35888.
- [62] R. Koerver, F. Walther, I. Aygün, J. Sann, C. Dietrich, W.G. Zeier, J. Janek, Redox-active cathode interphases in solid-state batteries, *J. Mater. Chem. A* 5 (2017) 22750.
- [63] D.H.S. Tan, E.A. Wu, H. Nguyen, Z. Chen, M.A.T. Marple, J.-M. Doux, X. Wang, H. Yang, A. Banerjee, Y.S. Meng, Elucidating reversible electrochemical redox of Li<sub>6</sub>PS<sub>5</sub>Cl solid electrolyte, *ACS Energy Lett.* 4 (2019) 2418.